



HAL
open science

The cadDX operon contributes to cadmium resistance, oxidative stress resistance, and virulence in zoonotic streptococci

Xinchi Zhu, Zijing Liang, Jiale Ma, Jinhu Huang, Liping Wang, Huochun Yao,
Zongfu Wu

► To cite this version:

Xinchi Zhu, Zijing Liang, Jiale Ma, Jinhu Huang, Liping Wang, et al.. The cadDX operon contributes to cadmium resistance, oxidative stress resistance, and virulence in zoonotic streptococci. *Veterinary Research*, 2024, 55 (1), pp.119. 10.1186/s13567-024-01371-1 . hal-04713789

HAL Id: hal-04713789

<https://hal.science/hal-04713789v1>

Submitted on 30 Sep 2024

HAL is a multi-disciplinary open access archive for the deposit and dissemination of scientific research documents, whether they are published or not. The documents may come from teaching and research institutions in France or abroad, or from public or private research centers.

L'archive ouverte pluridisciplinaire **HAL**, est destinée au dépôt et à la diffusion de documents scientifiques de niveau recherche, publiés ou non, émanant des établissements d'enseignement et de recherche français ou étrangers, des laboratoires publics ou privés.

RESEARCH ARTICLE

Open Access



The *cadDX* operon contributes to cadmium resistance, oxidative stress resistance, and virulence in zoonotic streptococci

Xinchi Zhu^{1,2,3}, Zijiang Liang^{1,2,3}, Jiale Ma^{1,2,3}, Jinhu Huang¹, Liping Wang¹, Huochun Yao^{1,2,3} and Zongfu Wu^{1,2,3,4*} 

Abstract

Mobile genetic elements (MGEs) enable bacteria to acquire novel genes and traits. However, the functions of cargo genes within MGEs remain poorly understood. The cadmium resistance operon *cadDX* is present in many gram-positive bacteria. Although *cadDX* has been reported to be involved in metal detoxification, its regulatory mechanisms and functions in bacterial pathogenesis are poorly understood. This study revealed that *cadDX* contributes to cadmium resistance, oxidative stress resistance, and virulence in *Streptococcus suis*, an important zoonotic pathogen in pigs and humans. CadX represses *cadD* expression by binding to the *cadDX* promoter. Notably, *cadX* responds to H₂O₂ stress through an additional promoter within the *cadDX* operon, mitigating the harmful effect of excessive *cadD* expression during oxidative stress. *cadDX* resides within an 11 K integrative and mobilizable element that can autonomously form circular structures. Moreover, *cadDX* is found in diverse MGEs, accounting for its widespread distribution across various bacteria, especially among pathogenic streptococci. Transferring *cadDX* into another zoonotic pathogen, *Streptococcus agalactiae*, results in similar phenotypes, including resistance to cadmium and oxidative stresses and increased virulence of *S. agalactiae* in mice. The new functions and regulatory mechanisms of *cadDX* shed light on the importance of the *cadDX* system in driving evolutionary adaptations and survival strategies across diverse gram-positive bacteria.

Keywords *Streptococcus suis*, *Streptococcus agalactiae*, mobile genetic elements, oxidative stress response, cadmium resistance, bacterial virulence

Introduction

Bacteria can acquire new genes via mobile genetic elements (MGEs), conferring additional attributes, including resistance to antibiotics and heavy metals, toxin production, and the ability to metabolize a wide range of compounds [1–4]. This process enables bacteria to adapt quickly to environmental stresses and promotes evolutionary innovation [5, 6]. The cadmium resistance operon *cadDX* comprises a P-type ATPase CadD and a member of the ArsR family transcriptional repressor CadX, which is crucial in conferring cadmium resistance in gram-positive bacteria. *cadDX* has been reported to be a plasmid-borne system in various bacteria [7–11].

Handling editor: Marcelo Gottschalk.

*Correspondence:

Zongfu Wu
wuzongfu@njau.edu.cn

¹ MOE Joint International Research Laboratory of Animal Health and Food Safety, College of Veterinary Medicine, Nanjing Agricultural University, Nanjing 210014, China

² Key Lab of Animal Bacteriology, Ministry of Agriculture, Nanjing 210014, China

³ WOA Reference Lab for Swine Streptococcosis, Nanjing 210014, China

⁴ Guangdong Provincial Key Laboratory of Research On the Technology of Pig Breeding and Pig Disease Prevention, Guangzhou 511400, China



© The Author(s) 2024. **Open Access** This article is licensed under a Creative Commons Attribution 4.0 International License, which permits use, sharing, adaptation, distribution and reproduction in any medium or format, as long as you give appropriate credit to the original author(s) and the source, provide a link to the Creative Commons licence, and indicate if changes were made. The images or other third party material in this article are included in the article's Creative Commons licence, unless indicated otherwise in a credit line to the material. If material is not included in the article's Creative Commons licence and your intended use is not permitted by statutory regulation or exceeds the permitted use, you will need to obtain permission directly from the copyright holder. To view a copy of this licence, visit <http://creativecommons.org/licenses/by/4.0/>. The Creative Commons Public Domain Dedication waiver (<http://creativecommons.org/publicdomain/zero/1.0/>) applies to the data made available in this article, unless otherwise stated in a credit line to the data.

In *Staphylococcus aureus* pI258, CadD functions as an energy-dependent efflux pump, increasing the minimum inhibitory concentration (MIC) of cadmium (Cd^{2+}) by approximately 1000-fold [8], whereas CadX regulates the transcription of *cadD* by binding to its promoter [11]. In the plasmid pLUG10 of *Staphylococcus lugdunensis*, a mutation in either *cadD* (also called *cadB*) or *cadX* reduces cadmium resistance, indicating that both genes are required for full cadmium resistance [7]. In *Streptococcus salivarius* 57. I, *cadD* is responsible for resistance to Cd^{2+} and zinc (Zn^{2+}), whereas CadX senses Cd^{2+} or Zn^{2+} and negatively regulates *cadD* expression [12]. A recent study on *Streptococcus agalactiae* reported that *cadD* is involved in the detoxification of metals, such as Zn^{2+} , Cd^{2+} , copper (Cu^{2+}), cobalt (Co^{2+}), and nickel (Ni^{2+}), and promotes immune evasion and bacterial colonization in pregnant hosts [13]. However, the regulatory mechanisms and functions of *cadDX* in bacterial pathogenesis are poorly understood.

Streptococcus suis is a pathogen capable of causing systemic diseases such as septicemia and meningitis in pigs [14]. It is also considered a zoonotic pathogen, posing a risk for humans with close contact with infected pigs or contaminated by-products [15, 16]. In this study, we revealed that *cadDX* contributes to cadmium resistance, oxidative stress resistance, and virulence in *S. suis*. Notably, *cadX* possesses its own promoter and promotes oxidative stress by preventing excessive expression of *cadD*, which harms *S. suis* survival during oxidative stress. Additionally, *cadDX* exists within an 11 K integrative and mobilizable element (IME) that can autonomously form circular structures in *S. suis*. Furthermore, we found that *cadDX* also confers resistance to cadmium and oxidative stresses and enhances the virulence of *S. agalactiae*, extending its phenotypic effects to different bacterial hosts.

Materials and methods

Bacterial strains and culture conditions

All strains and plasmids used in this study are listed in Additional file 1. *S. suis* and *S. agalactiae* strains were cultured in Todd-Hewitt broth (THB, Becton Dickinson, USA) and plated on THB agar (THA) medium containing 6% (vol/vol) sheep blood at 37 °C with 5% CO_2 . *Escherichia coli* strains were grown in Luria–Bertani (LB; Becton Dickinson, USA) broth at 37 °C. The following antibiotics were added as needed: spectinomycin (Macklin, China) at 50 $\mu\text{g}/\text{mL}$ for *E. coli*, 100 $\mu\text{g}/\text{mL}$ for *S. suis*, and kanamycin (Macklin, China) at 50 $\mu\text{g}/\text{mL}$ for *E. coli*. The metal salts, including ZnCl_2 , CdCl_2 , CuSO_4 , MnCl_2 , MgCl_2 , or NiCl_2 (Sinopharm Chemical Reagent Co. Ltd., Shanghai, China), were dissolved in deionized water to prepare metal stock solutions.

Polymerase chain reaction (PCR)

The DNA fragment was amplified by PCR using 2×Phanta Max Master Mix (Vazyme, Nanjing, China). The PCR mixture, with a final volume of 50 μL , contained 25 μL of 2×Phanta Max Master Mix, 1 μL of each 10 μM primer, 50 ng of genomic DNA, and ddH_2O . The PCR protocol included initial denaturation at 95 °C for 5 min, followed by 35 cycles of denaturation at 95 °C for 15 s, annealing at 55 °C for 15 s, and extension at 72 °C for 30 s. A final extension was performed at 72 °C for 5 min in an Applied Biosystems™ 2720 Thermal Cycler (Thermo Fisher Scientific, USA). The PCR products were electrophoresed on a 1% agarose gel stained with Goldview (Biosharp, China) Nucleic Acid Stain and scanned using a ChemiDoc XRS+ System (Bio-Rad, USA).

Construction of deletion mutants and complemented strains

The gene loci of *cadX*, *cadD*, *permease*, and *FeoA* in the GZ0565 genome are *BFP66_RS01345*, *BFP66_RS01350*, *BFP66_RS01325*, and *BFP66_RS02660*, respectively. The *cadDX* deletion mutant (ΔcadDX) and the *permease* deletion mutant ($\Delta\text{permease}$) were generated using the natural transformation method following a previous study [17]. To complement *cadDX* (*C-cadDX*), *cadD* (*C-cadD*), or *cadX* (*C-cadX*) into ΔcadDX , PCR fragments containing either *cadDX* or *cadD* with the *cadDX* operon promoter or *cadX* with both the *cadDX* operon promoter and its own promoter were cloned and inserted into the pSET2 plasmid [18], respectively. The recombinant plasmid was then transformed into the ΔcadDX strain. To construct the *FeoA* overexpression strain, a PCR fragment containing *FeoA* with its own operon promoter was cloned and inserted into the pSET2 plasmid, and the recombinant plasmid was then transformed into the GZ0565 strain (WT). The plasmids pSET2, pSET2-*cadDX*, pSET2-*cadD*, or pSET2-*cadX* were subsequently transferred into *S. agalactiae* GD201008-001, resulting in the construction of *S. agalactiae*-pSET2, *S. agalactiae*-*cadDX*, *S. agalactiae*-*cadD*, or *S. agalactiae*-*cadX*, respectively. The plasmids pSET2 or pSET2-*cadDX* were transferred into a virulence-attenuated strain of *S. agalactiae* GD201008-001 with deletion of the *CRISPR* locus ($\Delta\text{CRISPR}_{S,a}$) [19], resulting in the construction of $\Delta\text{CRISPR}_{S,a}$ -pSET2 or $\Delta\text{CRISPR}_{S,a}$ -*cadDX*, respectively. All primers are provided in Additional file 2.

RNA extraction and transcriptome analysis

For transcriptome analysis, the WT and ΔcadDX were grown to the exponential phase ($\text{OD}_{600}=0.6$) in THB. Total RNA was extracted using the FastRNA Pro Blue Kit (MP Biomedicals, USA). All the RNA samples were

subsequently purified by DNase I (Takara, Dalian, China) digestion, phenol/chloroform extraction, and ethanol precipitation, as described in our previous study [20]. Two biological replicates were combined for each bacterium to create a sequencing sample, and two sequencing samples were prepared for both the WT and $\Delta cadDX$ groups. The RNA samples were sent to Genedenovo Technology (Guangzhou, China) for transcriptome analysis. Following the manufacturer's protocol, sequencing was performed using the Illumina HiSeq 2500 platform (Illumina, USA). The sequencing reads were aligned by Bowtie2 [21]. Gene expression was calculated via the fragments per kilobase of transcript per million mapped reads (FPKM) algorithm by expectation–maximization (RSEM) software, and differential expression analysis was conducted using edgeR [22, 23]. Significance thresholds of $p < 0.05$ and $|\log_2 \text{fold-change}| \geq 1.0$ were applied to identify differentially expressed genes (DEGs).

Real-time quantitative PCR (RT-qPCR)

To evaluate the expression of *cadD* and *cadX* in *S. suis* in response to various metals, *S. suis* GZ0565 was grown to the exponential phase ($OD_{600} = 0.6$) in THB and then divided into seven equal aliquots, supplemented with 15 μM CdCl_2 , 0.5 mM ZnCl_2 , 1 mM CuSO_4 , 1 mM MnCl_2 , 1 mM MgCl_2 , 1 mM NiCl_2 , or deionized water, respectively. The concentrations of these heavy metals were determined on the basis of several reports on the response of *S. suis* to metals, with slight modifications [24–27]. After 1 h of incubation, the cultures were centrifuged at 5000 g for 10 min at 4 °C to collect the bacterial pellets. Total RNA isolation was performed as described above.

Approximately 0.5 μg of RNA per sample was converted to cDNA using the HiScript III 1st Strand cDNA Synthesis Kit (+gDNA wiper) (Vazyme, Nanjing, China). Quantitative PCR was conducted using the Applied Biosystems QuantStudio 6 Flex system (Applied Biosystems, USA) with ChamQ Universal SYBR qPCR Master Mix (Vazyme, Nanjing, China). The primers used for RT-qPCR analysis are listed in Additional file 2, with the gene *BFP66_RS05620* (*parC*) serving as the internal control. The relative fold change was calculated using the $2^{-\Delta\Delta CT}$ method. At least three biological replicates were included for each experiment.

Growth curve and viability analyses

For growth curve analysis, *S. suis* was initially cultured overnight in THB. Then, they were diluted 1:100 in fresh THB or THB supplemented with different concentrations of CdCl_2 (7.5, 15, 20, and 30 μM), ZnCl_2 (0.25, 0.5, 1.0, and 2.0 mM), or CuSO_4 (0.25, 0.5, 1.0, and 2.0 mM) without spectinomycin. The concentrations of these heavy

metals were determined on the basis of our preliminary experiments, where high concentrations of CdCl_2 (≥ 50 μM), ZnCl_2 (≥ 5 mM), or CuSO_4 (≥ 5 mM) led to complete inhibition of growth, whereas low concentrations of CdCl_2 (≤ 5 μM), ZnCl_2 (≤ 0.2 mM), or CuSO_4 (≤ 0.2 mM) had no observed effect on the growth of *S. suis* strain GZ0565. For *S. agalactiae*, overnight cultures were diluted 1:100 in fresh THB or THB supplemented with 15 μM CdCl_2 without spectinomycin. The bacterial cultures were incubated in 96-well plates at 37 °C, and the optical density at 595 nm was monitored hourly using a microplate reader (Molecular Devices, USA). Additionally, the bacterial viability of *S. suis* was assessed at 6 h through serial dilution (10^{-1} to 10^{-5}) and plating onto THA plates overnight incubation. At least three biological replicates were included for each experiment.

Expression and purification of the CadX protein

To express the CadX homodimer, a linker sequence (GGGGSGGGGSGGGGS) was inserted between two identical CadX protein sequences and then ligated into the pET28a vector to produce pET28a-CadX, following a previously established protocol [28]. *E. coli* BL21(DE3) containing the expression plasmid was cultured in 200 mL of LB supplemented with kanamycin at 37 °C until the OD_{600} reached 0.4 to 0.6. Protein expression was induced by adding 1 mM IPTG, and the culture was incubated at 16 °C for 12 h. The cells were harvested by centrifugation (5000 g , 10 min, 4 °C) and resuspended in 25 mL of PBS. After sonication and centrifugation (13,000 g , 10 min, 4 °C), the supernatant was loaded onto a HisTrap HP column (GE Healthcare, USA) and washed with buffer A (20 mM phosphate buffer, pH 7.4; 500 mM NaCl; 20 mM imidazole). Proteins were eluted with buffer E (20 mM phosphate buffer, pH 7.4; 500 mM NaCl; 500 mM imidazole). The eluted fractions were analysed by a 12% SDS gel, and the concentration of the purified protein was measured by Pierce™ BCA protein assay kits (Thermo Fisher Scientific, USA).

Electrophoretic mobility shift assay (EMSA)

The promoter fragments of the target genes, as well as the 16S rRNA gene, were amplified by PCR with 2×Rapid Taq Master Mix (Vazyme, Nanjing, China) from the GZ0565 genome and purified using FastPure Gel DNA Extraction Mini Kit (Vazyme, Nanjing, China). The DNA probes and CadX recombinant protein were incubated in a 20 μL reaction mixture (10 mM Tris, 50 mM KCl, 1 mM MgCl_2 , 1 mM DTT, 0.05% Triton X-100, 2.5% glycerol, pH 7.5) at 37 °C for 30 min, followed by electrophoresis on a 6% native polyacrylamide gel in 0.5×TB buffer (44.5 mM Tris-base, 44.5 mM boric acid, pH 7.5) at 200 V for 45 min. To assess the effect of Cd^{2+} on the affinity of

CadX for the *cadDX* promoter region, the DNA probes and CadX recombinant protein were incubated in the presence of 2, 4, or 8 μM CdCl_2 . The gel was stained with Goldview (Biosharp, China) for 10 min and scanned using a ChemiDoc XRS⁺ System (Bio-Rad, USA).

β -galactosidase activity assay

The promoter fragments were amplified from the GZ0565 genome and ligated into the pTCV-*LacZ* reporter plasmid [29]. The recombinant plasmids were introduced into the WT and ΔcadDX strains. The β -galactosidase activity assay followed Miller's method with certain modifications [30]. The overnight cultures were diluted 1:100 in fresh THB and incubated at 37 °C with 5% CO_2 . When the exponential phase was reached, the OD_{600} was measured. Subsequently, 4 mL of each culture was concentrated to 400 μL , and the culture was transferred to precooled tubes on ice. Then, 25 μL of 4 \times Z-buffer (240 mM $\text{Na}_2\text{HPO}_4\cdot 2\text{H}_2\text{O}$, 160 mM $\text{NaH}_2\text{PO}_4\cdot 2\text{H}_2\text{O}$, 40 mM KCl, and 4 mM $\text{MgSO}_4\cdot 7\text{H}_2\text{O}$, pH 7.0) containing 50 mM β -mercaptoethanol and 4 μL of lysozyme (2.5 mg/mL) were added to the culture and incubated in a 37 °C water-bath for 30 min. Subsequently, 400 μL of 1 \times Z-buffer containing 2 mg/mL ONPG (O-nitrophenyl- β -d-galactopyranoside) was added, and the reaction continued to incubate in a 37 °C water-bath for 120 min. The reaction was terminated with 400 μL of 1 M Na_2CO_3 . After centrifugation, the supernatant was collected, and the optical density at 420 nm (OD_{420}) was measured. β -galactosidase activity was calculated according to the following formula:

$$\text{activity}[\text{MU}] = \frac{\text{OD}_{420} \times 1000 \times V_E[\mu\text{L}]}{V_s[\mu\text{L}] \times \text{RT}[\text{min}] \times \text{OD}_{600}}$$

where MU = Miller units, V_E = end volume, RT = reaction time, and V_s = volume of each sample. At least three biological replicates were included for each experiment.

5'-RACE

To identify the transcriptional start site (TSS) of *cadX*, the SMARTer RACE 5'/3' cDNA amplification kit (Takara, Dalian, China) was used according to the manufacturer's instructions. Total RNA was extracted and converted to cDNA to capture the 5' RNA ends. 5'-RACE was performed using nested PCR, which involved two rounds of PCR amplification of the cDNA. The first round of PCR was conducted with the specific primer GSP-*cadX* and the Universal Primer Short. The product was then diluted and subjected to a second round of PCR using NGSP-*cadX* and the Universal Primer Short. The PCR products were separated on 1.5% agarose gels and purified by a FastPure Gel DNA Extraction Mini Kit (Vazyme, Nanjing, China). The purified fragments were ligated into the

linearized pMD19T vector (Takara, Dalian, China). After sequencing (Sangon Biotech, Shanghai, China) and alignment to the GZ0565 genome, the 5' end of *cadX* was identified. The primers used are listed in Additional file 2.

Oxidative stress assay

To evaluate the role of *cadDX* in the oxidative stress response, bacteria were challenged with H_2O_2 . All the strains were cultured to the exponential phase ($\text{OD}_{600}=0.6$). H_2O_2 was subsequently added to achieve a final concentration of 25 mM in THB. After incubation at 37 °C for 25 min, bacterial counts were determined by spreading serial dilutions on THA plates. The survival rate at each time point was calculated as CFU at 25 min/CFU at time point 0. At least three biological replicates were included for each experiment.

Protein sequence alignment and phylogenetic analysis

The CadX and CadD protein sequences were aligned using BLASTp. The selected homologous sequences were further aligned using Clustal Omega [31], and a maximum-likelihood phylogenetic tree was constructed using MEGA X software [32]. The serotypes of 191 *S. suis* strains, which were randomly chosen from the BLASTp results, were analysed on the basis of their variation in capsular polysaccharide (CPS) antigenicity [33]. Information on *S. suis* strains with *cadDX* used for serotype distributions and bacteria with *cadDX* used for phylogenetic analysis is provided in Additional file 3 and Additional file 4, respectively.

Determination of viable bacteria in organs

The virulence of *S. suis* (WT, ΔcadDX , and *C-cadDX*) and *S. agalactiae* ($\Delta\text{CRISPR}_{S_a}$ -pSET2 and $\Delta\text{CRISPR}_{S_a}$ -*cadDX*) was assessed in mice. Mouse infection was carried out at the Laboratory Animal Center of Nanjing Agricultural University with the approval of the institution's ethics committee (permit number SYXK (Su) 2021-0086). Bacteria were cultured to the exponential phase ($\text{OD}_{600}=0.6$), washed twice with PBS, and used for infection in six-week-old SPF CD1 female mice (SiPeiFu Biotechnology, Shanghai, China), with six mice per group for *S. suis* and five mice per group for *S. agalactiae*. For *S. suis*, the mice were intraperitoneally injected with 1.5×10^8 CFU of *S. suis* following a previously established protocol [34]. For *S. agalactiae*, the mice were intraperitoneally injected with 1.0×10^2 CFU of *S. agalactiae* due to its high virulence in the mouse infection model, as reported in a published study [19]. All the mice were euthanized at 24 h post-infection. Blood samples (20 μL) were collected from the heart; liver, kidney, and brain samples were taken, weighed, suspended in PBS, and homogenized. The number of viable bacteria in organs

and blood was determined by plating serial dilutions onto THA.

Statistical analyses

For experiments with three groups or more than three groups, comparisons between groups were conducted via one-way ANOVA followed by Dunnett's multiple comparisons test. For experiments with only two groups, such as the β -galactosidase activity assay and determination of *S. agalactiae* in organs, unpaired two-tailed Student's *t* tests were used. Before performing unpaired two-tailed Student's *t* tests, we tested for equal variances via an *F* test. Statistical analyses were performed using GraphPad Prism version 8 software. The data are presented as mean \pm SD, and statistical significance was set at $p < 0.05$.

Results

Expression of *cadD* and *cadX* in *S. suis* under different metal conditions

To explore the involvement of *cadDX* in the response of *S. suis* to different metals, RT-qPCR was used to analyse the expression of *cadD* and *cadX* in the WT strain treated with various metals. The expression of *cadD* in *S. suis* was upregulated 5.23-fold in response to 15 μ M CdCl₂, 3.97-fold in response to 0.5 mM ZnCl₂, and 8.35-fold in response to 1 mM CuSO₄ (Figure 1). Similarly, the expression of *cadX* in *S. suis* was upregulated 6.27-fold in response to 15 μ M CdCl₂, 4.17-fold in response to 0.5 mM ZnCl₂, and 8.20-fold in response to 1 mM CuSO₄ (Figure 1). In contrast, the expression of *cadD* and *cadX* was not induced by 1 mM MnCl₂, 1 mM MgCl₂, or 1 mM

NiCl₂ (Figure 1). These results suggest that *cadDX* may be involved in the response of *S. suis* to stress induced by Cd²⁺, Zn²⁺, or Cu²⁺.

cadDX protects *S. suis* against cadmium stress

The growth of the WT, Δ *cadDX*, *C-cadDX*, *C-cadD*, and *C-cadX* strains in THB media supplemented with different concentrations of CdCl₂ (7.5, 15, 20, or 30 μ M), ZnCl₂ (0.25, 0.5, 1.0, or 2.0 mM), or CuSO₄ (0.25, 0.5, 1.0, or 2.0 mM) was evaluated to further investigate the role of *cadDX* in the *S. suis* response to excessive metals. All the strains exhibited similar growth in THB (Figure 2A). When 7.5 μ M CdCl₂ was added to the THB, the *C-cadDX* strain grew better than the Δ *cadDX*, *C-cadD*, and *C-cadX* strains did (Figure 2B). With the addition of 15 or 20 μ M CdCl₂, the WT, *C-cadD*, and *C-cadDX* strains demonstrated superior growth compared with the Δ *cadDX* and *C-cadX* strains (Figures 2C, D). At 30 μ M CdCl₂, the *C-cadD* and *C-cadDX* strains exhibited better growth than the WT, Δ *cadDX*, and *C-cadX* strains did (Figure 2E). Bacterial viability was determined to further evaluate the role of *cadDX* in resistance to Cd²⁺ (Figures 2F–J). Following a 6-h treatment with 15, 20, or 30 μ M CdCl₂, the Δ *cadDX* and *C-cadX* strains formed fewer colonies than the WT, *C-cadD*, and *C-cadDX* strains did. However, all strains exhibited similar growth curves under ZnCl₂ or CuSO₄ conditions (0.25, 0.5, 1.0, or 2.0 mM), indicating that *cadDX* does not play a pivotal role in the response to Zn²⁺ or Cu²⁺ stress in *S. suis* (Additional files 5A–H).

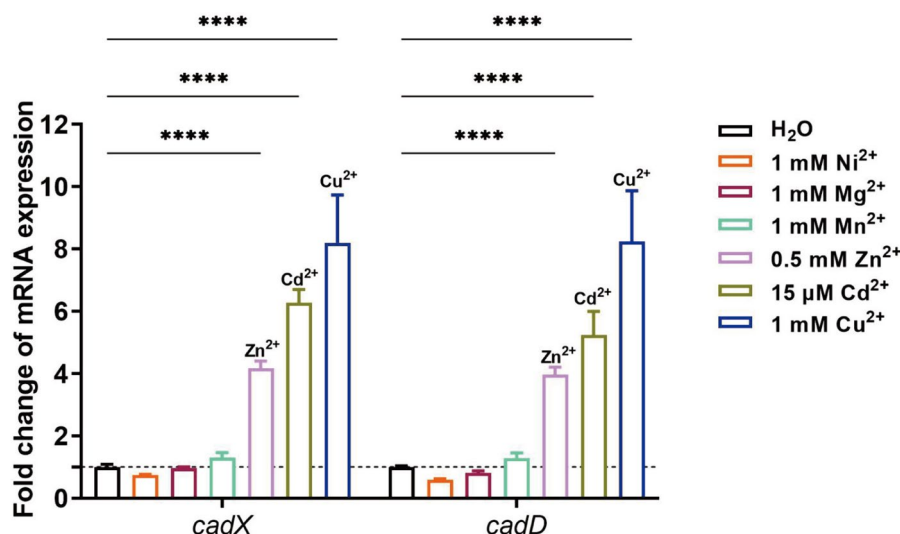


Figure 1 Expression of *cadD* and *cadX* in *S. suis* under different metal conditions. The expression of *cadD* and *cadX* in the WT strain was determined under H₂O (control) or different metal conditions (15 μ M CdCl₂, 0.5 mM ZnCl₂, 1 mM CuSO₄, 1 mM MnCl₂, 1 mM MgCl₂, and 1 mM NiCl₂). Data are presented as mean \pm SD, and asterisks indicate significantly different values (**** indicates $p < 0.0001$).

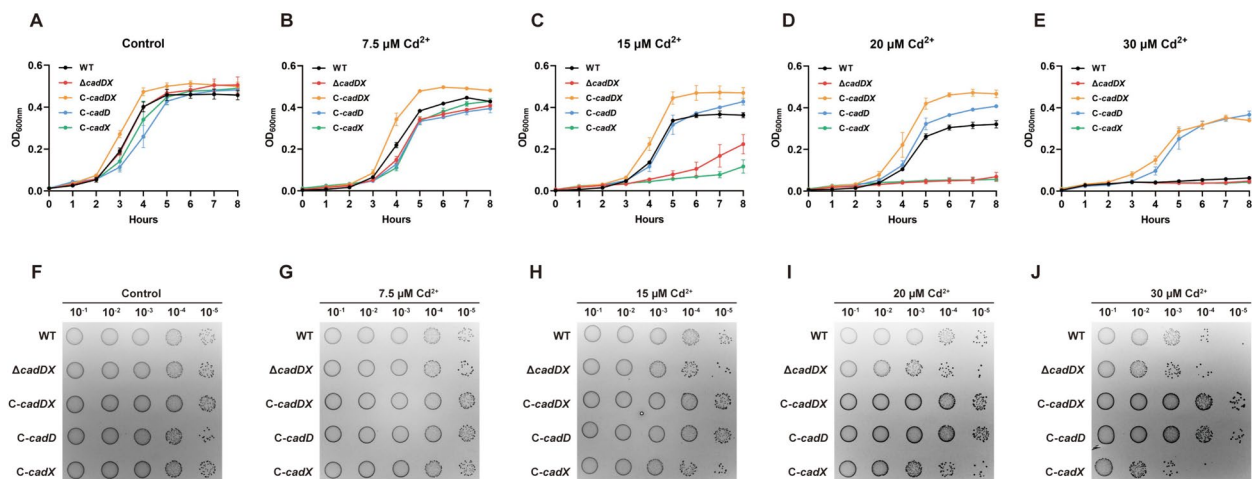


Figure 2 *cadDX* protects *S. suis* against cadmium stress. **A–E** Growth curves of WT, $\Delta cadDX$, *C-cadDX*, *C-cadD*, and *C-cadX* in THB (Control) or THB supplemented with various concentrations of $CdCl_2$ (7.5, 15, 20, and 30 μM). **F–J** Bacterial viability of the WT, $\Delta cadDX$, *C-cadDX*, *C-cadD*, and *C-cadX* strains after 6 h of culture in THB (control) or THB supplemented with various concentrations of $CdCl_2$ (7.5, 15, 20, and 30 μM).

Autoregulatory mechanism of *cadDX* in cadmium resistance

To elucidate the regulatory mechanism of *cadDX* in cadmium resistance, we initially expressed, purified the CadX protein, and amplified a DNA fragment containing the *cadDX* promoter. We then assessed the interaction between the CadX protein and the *cadDX* promoter region by EMSA. The EMSA results revealed that CadX directly binds to the *cadDX* promoter region (Figure 3A). Moreover, the activity of β -galactosidase under the control of the *cadDX* promoter was significantly greater in the $\Delta cadDX$ strain than in the WT strain (Figure 3B). Additionally, a previous study reported that the affinity of CadX for the *cadDX* promoter region was influenced by the presence of Cd^{2+} [12]. Consistent with these findings, the EMSA results indicated that the affinity of CadX for the *cadDX* promoter region was significantly reduced in the presence of Cd^{2+} (Figure 3C).

cadDX contributes to oxidative stress resistance

In our recent study, *cadD* (2.4-fold change) and *cadX* (3.4-fold change) were found to be upregulated in response to H_2O_2 stress compared with those in THB medium by transcriptome analysis, suggesting potential functions of *cadDX* under oxidative stress [35]. Thus, we evaluated the survival of the WT, $\Delta cadDX$, *C-cadDX*, *C-cadD*, and *C-cadX* strains under H_2O_2 conditions. The results revealed that, compared with the WT and *C-cadDX* strains, the $\Delta cadDX$ strain presented a significantly lower survival rate after H_2O_2 treatment (Figure 4A). Additionally, *cadX* complementation alone in $\Delta cadDX$ restored its resistance to H_2O_2 to the WT level, while *C-cadD* further reduced resistance to H_2O_2 (Figure 4A). Compared

with that of *C-cadDX*, *cadD* expression was substantially increased in *C-cadD* because of the absence of *cadX* (Additional file 6A). Given the divergent expression patterns of *cadD* and *cadX* during oxidative stress (2.4-fold and 3.4-fold changes, respectively), we hypothesized that *cadX* might have an additional promoter within the *cadDX* operon. To explore this hypothesis, we conducted a 5' RACE analysis to pinpoint the TSS of *cadX* (Additional file 6B). We identified an additional TSS at -56 relative to the *cadX* start codon (Figure 4B and Additional file 6C). However, we observed no interaction between CadX and its own promoter (Additional file 6D). The activity of β -galactosidase under the control of the *cadX* promoter in the $\Delta cadDX$ strain was comparable to that in the WT strain (Additional file 6E).

To explore the influence of the *cadDX* operon on gene expression in *S. suis*, we conducted transcriptome analysis of the WT and $\Delta cadDX$ strain. In the absence of *cadDX*, we identified 65 DEGs, consisting of 42 upregulated and 23 downregulated genes (Figure 4C) (Additional file 7). To confirm the reliability of the transcriptome data, seven upregulated and six downregulated DEGs were randomly selected for further analysis. The transcription levels of these genes were consistent with those obtained from the transcriptome analysis (Additional file 8), indicating the reliability of the transcriptome data. The 65 DEGs are involved in various biological processes, including fatty acid biosynthesis, carbohydrate transport and metabolism, and metal ion transport. Notably, among these DEGs, only *permease* (encoded by *BFP66_RS01325*) and *integrase* (encoded by *BFP66_RS01340*) were located within the 11 K IME (Figure 4C), which suggests that *cadDX*

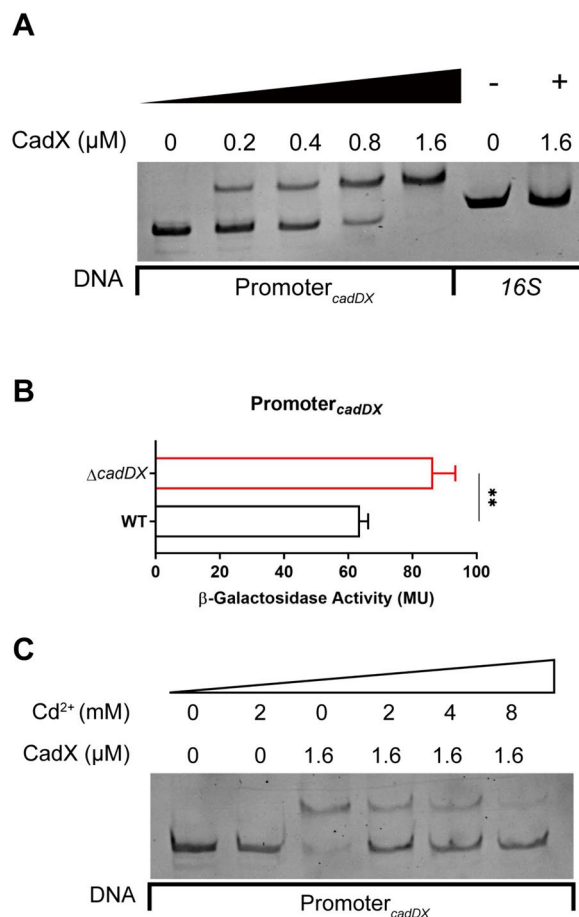


Figure 3 Autoregulatory mechanism of *cadDX* in cadmium resistance. **A** CadX directly binds to the *cadDX* promoter. **B** The activity of β-galactosidase under the control of the *cadDX* promoter in the WT and $\Delta cadDX$ strains. **C** Cd²⁺ reduces the affinity of CadX for the *cadDX* promoter. Data are presented as mean \pm SD, and asterisks indicate significantly different values (**** indicates $p < 0.01$).

mainly affects the expression of bacterial genomic genes outside the 11K IME. As shown in Additional file 7, six genes related to the PTS transporter system (encoded by *BFP66_RS02205*, *BFP66_RS02210*, *BFP66_RS02215*, *BFP66_RS02220*, *BFP66_RS02225*, and *BFP66_RS02230*) were upregulated in $\Delta cadDX$. The genes associated with fatty acid biosynthesis (encoded by *BFP66_RS08345*, *BFP66_RS08350*, and *BFP66_RS08355*) were downregulated. We also found that ferrous iron transport *FeoA* (encoded by *BFP66_RS02660*) was upregulated and that *permease* was downregulated in $\Delta cadDX$. Furthermore, the activity of β-galactosidase under the control of the promoter of *Fab* (*BFP66_RS08355*, the first gene of the operon involved in fatty acid biosynthesis) or *permease* was

decreased in $\Delta cadDX$ (Additional files 9A and B). In contrast, the activity of β-galactosidase under the control of the promoter of *PTS* (*BFP66_RS02205*, the first gene of the operon involved in the PTS transporter system) or *FeoA* was increased (Additional files 9C and D). However, CadX did not directly bind to the promoters of these genes (Additional files 9E–H). Furthermore, we selected *permease* and *FeoA* for further analysis on the basis of their functions, which may be involved in oxidative stress resistance. After the *permease* deletion strain ($\Delta permease$) and the *FeoA* overexpression strain (OE-*FeoA*) were subjected to H₂O₂ treatment, both strains presented significantly lower survival rates than the WT strain did (Additional file 10).

cadDX contributes to *S. suis* virulence in a mouse infection model

Given the role of *cadDX* in alleviating oxidative stress in *S. suis*, we investigated its contribution to *S. suis* virulence in a mouse model. Compared with those in the WT and *C-cadDX* infection groups, the number of $\Delta cadDX$ bacteria in the blood, brain, kidney, liver, and spleen was significantly lower (Figures 5A–E).

Characterization of the 11K IME in *S. suis* GZ0565

In the *S. suis* virulent strain GZ0565, we identified the *cadDX* operon within an 11 K IME that contains characteristics of IME, including site-specific integrases, replication proteins, and translocases (Figure 6A). Direct repeats (*attL* and *attR*) were detected on both sides of this IME, suggesting the potential for circularization of the 11 K IME and subsequent transfer to new hosts. We designed two pairs of primers to assess their circularization ability. We confirmed that the 11 K IME could excise from the bacterial chromosome, forming an extrachromosomal circular molecule (Figures 6B, C). Subsequent sequence analysis validated the expected structures of *attR* (Figure 6D) and *attL* (Figure 6E) generated during site-specific excision.

Distribution of *cadDX* in bacteria

Genome analysis revealed the prevalence of the *cadDX* operon in diverse *S. suis* serotypes, including ten serotypes (serotypes 2, 4, 5, 7, 9, 14, 16, 21, 24, and 31) known to cause human infections (Figure 7A). Except for the gram-negative bacteria *Neisseria*, where *cadD* is an orphan gene, the *cadDX* operon is present in various gram-positive bacteria, including *Streptococcus*, *Lactococcus*, *Enterococcus*, *Staphylococcus*, *Listeria*, *Ligilactobacillus*, and *Gemella*. Among these gram-positive bacteria, pathogenic streptococci such as *Streptococcus pyogenes*, *Streptococcus dysgalactiae*, *Streptococcus equi* subsp. *zooepidemicus*, and *S. agalactiae* present the

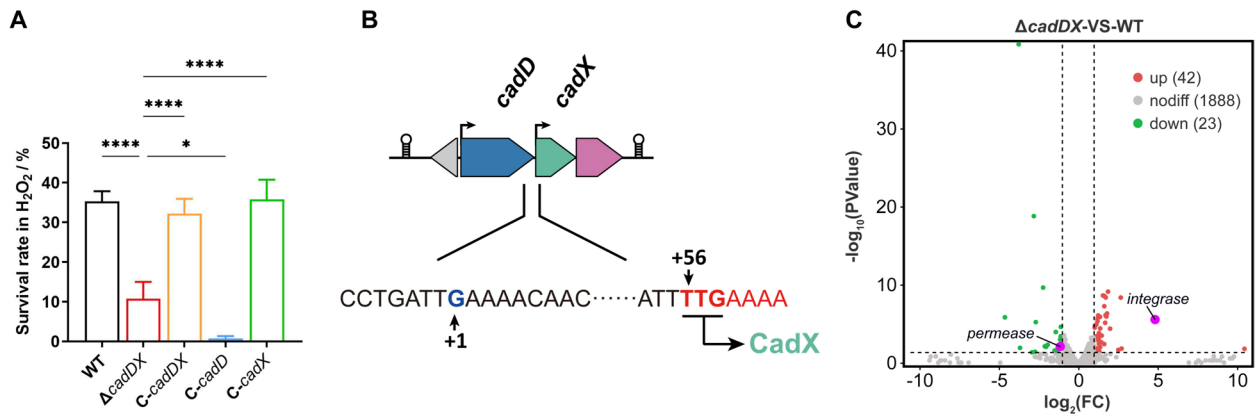


Figure 4 *cadDX* contributes to oxidative stress resistance. **A** Survival rates of the WT, $\Delta cadDX$, *C-cadDX*, *C-cadD*, and *C-cadX* strains under H₂O₂ stress conditions. **B** An additional promoter of *cadX* inside the *cadDX* operon. “TTG” is the start codon of *CadX*. “+ 1” indicates the position of the identified additional TSS. **C** Volcano plot demonstrating DEGs in the $\Delta cadDX$ strain compared with the WT strain by transcriptome analysis. The cut-off for enrichment was set at $|\log_2(FC)| \geq 1.0$ and a *p* value < 0.05, as indicated by the dashed lines. The upregulated genes are marked with red dots, the downregulated genes are marked with green dots, and the DEGs within the 11K IME are marked with purple dots. Data are presented as mean \pm SD, and asterisks indicate significantly different values (“*” and “****” indicate *p* < 0.05 and *p* < 0.0001, respectively).

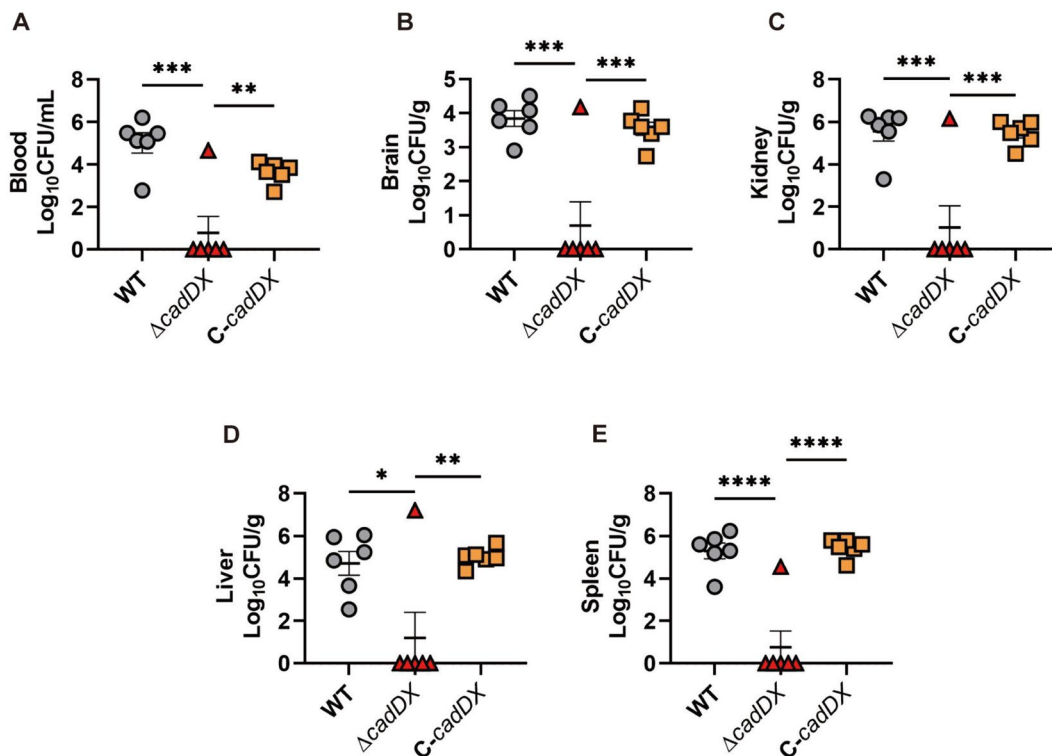


Figure 5 *cadDX* contributes to *S. suis* virulence in a mouse infection model. Six mice per group were injected intraperitoneally with 1.5×10^8 CFU of the WT, $\Delta cadDX$, or *C-cadDX* strains. All the mice were euthanized at 24 h post-infection. Bacteria from the blood (**A**), brain (**B**), kidney (**C**), liver (**D**), and spleen (**E**) were plated onto THA, and colonies are expressed as Log₁₀CFU/g or Log₁₀CFU/mL. Data are presented as mean \pm SD, and asterisks indicate significantly different values (“*”, “***”, “****”, and “*****” indicate *p* < 0.05, *p* < 0.01, *p* < 0.001, and *p* < 0.0001, respectively).

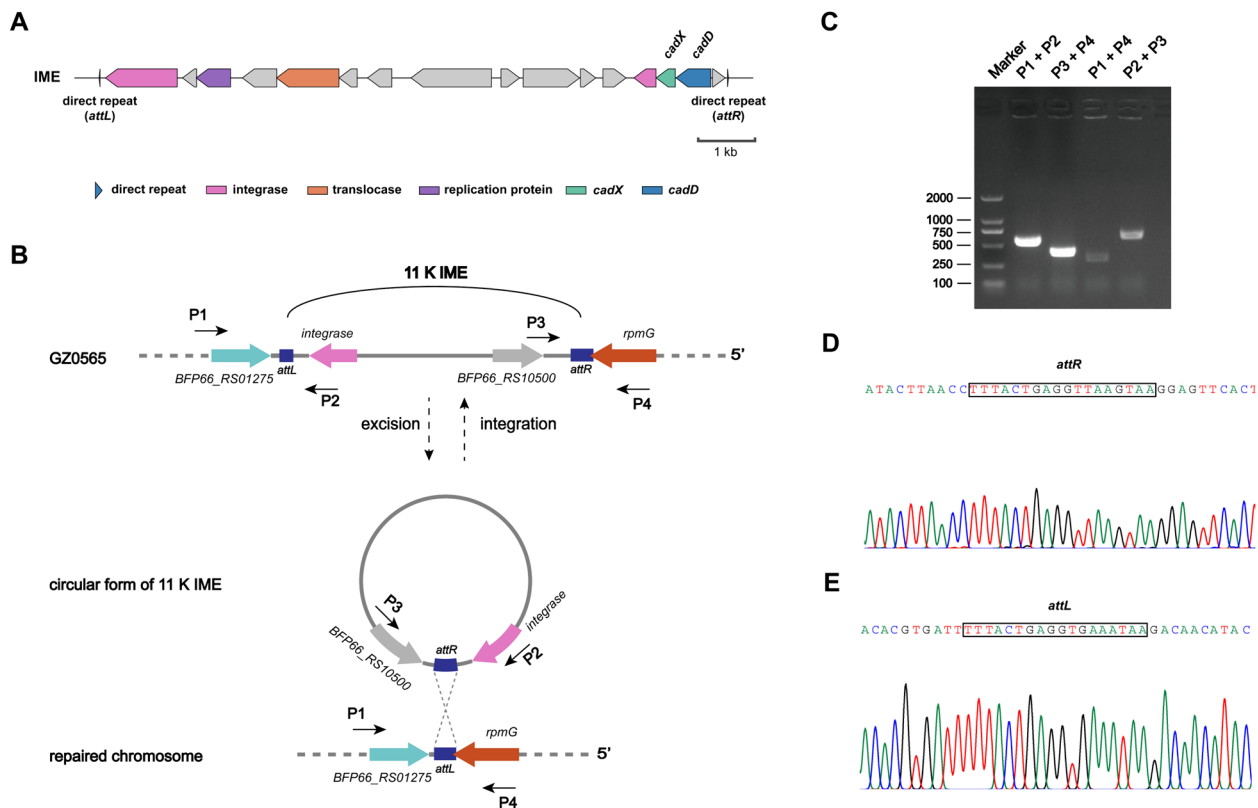


Figure 6 Characterization of the 11K ICE in *S. suis* GZ0565. **A** The 11K ICE contains direct repeats, a site-specific integrase, a replication protein, and a translocase. **B** Illustration of the site-specific integration and excision of the 11K ICE. The locations and orientations of the primers used for detecting integrated and excised 11K are indicated by arrows. **C** Detection of a circular extrachromosomal form of the 11K ICE by PCR analysis. **D** Sequencing chromatogram of PCR products amplified with the primer pair P2/P3 showing the *attR* site (boxed). **E** Sequencing chromatogram of PCR products amplified with the primer pair P1/P4 showing the *attL* site (box) upon 11K ICE excision.

highest prevalence of the *cadDX* operon (Figure 7B). The widespread distribution of *cadDX* indicates horizontal transfer across diverse bacteria. Importantly, this horizontal transfer of *cadDX* can occur through various vectors. In *S. suis* strain WUSS351, *cadDX* resides within a predicted 10 K ICE containing recombinase, which differs from its location in the *S. suis* strain GZ0565. Similarly, another 32 K genomic island with an integrase and transposase also contains *cadDX* in the *S. suis* strain NSUI002. A similar trend was observed in *S. agalactiae* strains NJ1606 and 32790-3A, where *cadDX* was identified in two different ICEs along with several genes associated with horizontal transfer, such as conjugal transfer proteins, translocases, replication proteins, and integrases. Additionally, *cadDX* was found within a prophage containing recombinase in *S. agalactiae* strain B508 (Figure 7C). Overall, these findings underscore the significant variability in the distribution and genetic context of *cadDX* among gram-positive bacteria, especially pathogenic streptococci. This diversity has substantial

implications for the evolution and functional roles of *cadDX* across distinct bacterial populations.

cadDX* confers resistance to cadmium and oxidative stresses and enhances virulence in *S. agalactiae

To investigate whether *cadDX* could confer similar functions in recipient bacteria lacking this operon, we introduced *cadDX* into the *S. agalactiae* strain GD201008-001 using the pSET2 plasmid. In THB media, *S. agalactiae*-pSET2, *S. agalactiae*-*cadDX*, *S. agalactiae*-*cadD*, and *S. agalactiae*-*cadX* displayed comparable growth curves (Figure 8A). However, when cultured in THB containing 15 μM CdCl_2 , the growth of *S. agalactiae*-*cadD* and *S. agalactiae*-*cadDX* were notably greater than those of *S. agalactiae*-pSET2 and *S. agalactiae*-*cadX* (Figure 8B). Similarly, the survival rates of *S. agalactiae*-*cadX* and *S. agalactiae*-*cadDX* increased under H_2O_2 conditions compared with those of *S. agalactiae*-pSET2 (Figure 8C). Moreover, compared with *S. agalactiae*-pSET2, *S. agalactiae*-*cadD* also exhibited increased sensitivity to H_2O_2 . Notably, owing to the high virulence of the *S.*

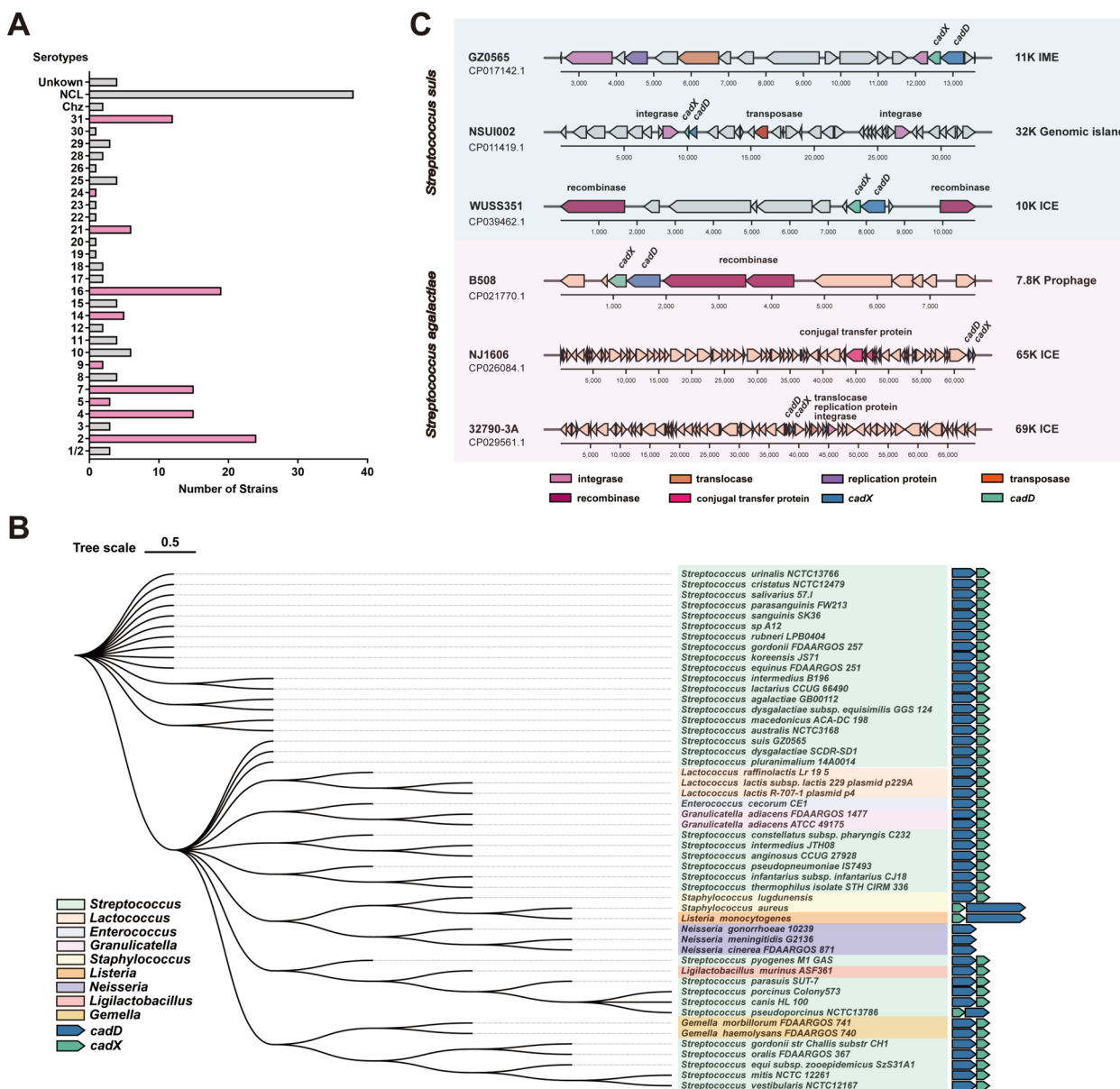


Figure 7 Distribution of *cadDX* in bacteria. **A** The presence of *cadDX* in different *S. suis* serotypes. **B** The presence of *cadDX* in different gram-positive bacteria, including *Streptococcus*, *Lactococcus*, *Enterococcus*, *Staphylococcus*, *Listeria*, *Ligilactobacillus*, and *Gemella*, and the gram-negative bacterium *Neisseria*. **C** *cadDX* within different vectors in *S. suis* and *S. agalactiae*.

agalactiae strain GD201008-001 in a mouse infection model, with a 50% lethal dose value of less than 10 CFU, we employed the virulence-attenuated strain $\Delta CRISPR_{S,a}$ as a background to assess the contributions of *cadDX* to *S. agalactiae* virulence [19, 36]. Compared with those in the $\Delta CRISPR_{S,a}$ -pSET2 infection group, the number of bacteria in the blood, brain, kidney, and liver in the $\Delta CRISPR_{S,a}$ -*cadDX* infection group was significantly greater (Figures 8D–G), although no significant difference was observed in the spleen (Additional file 11).

These results demonstrate that *cadDX* also confers resistance to cadmium and oxidative stresses and enhances virulence in *S. agalactiae*.

Discussion

Cadmium, a prevalent environmental pollutant, is found worldwide, particularly in areas near water resources [37]. It is a frequent contaminant in animal feed additives, often appearing as an impurity in mineral supplements such as phosphates, zinc sulfate, and zinc oxide;

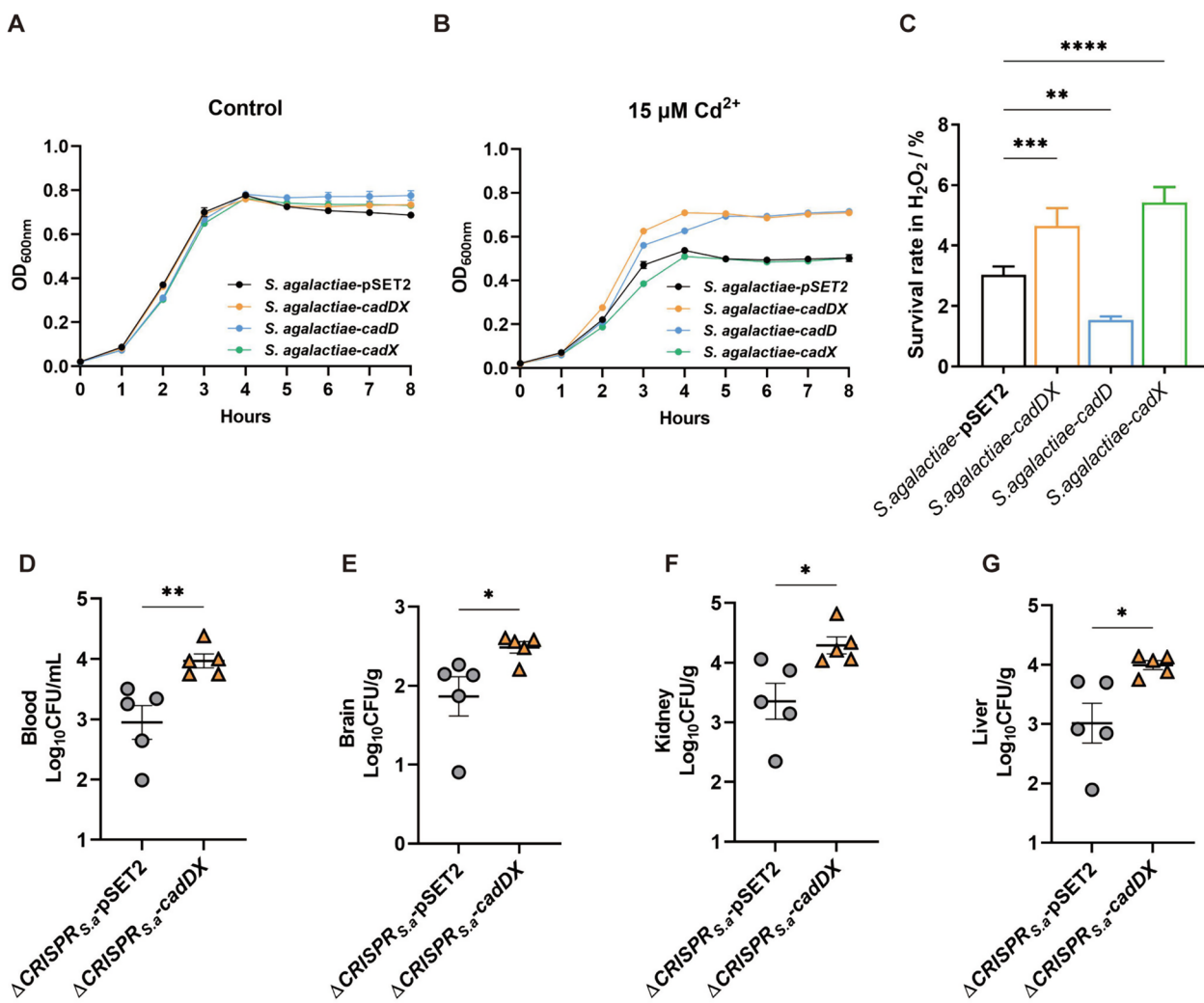


Figure 8 *cadDX* confers resistance to cadmium and oxidative stress and enhances virulence in *S. agalactiae*. **A, B** Growth curves of *S. agalactiae*-pSET2, *S. agalactiae-cadDX*, *S. agalactiae-cadD*, and *S. agalactiae-cadX* cultured in THB (control) or THB supplemented with 15 μM CdCl₂. **C** Survival rates of *S. agalactiae*-pSET2, *S. agalactiae-cadDX*, *S. agalactiae-cadD*, and *S. agalactiae-cadX* under H₂O₂ stress conditions. Five mice per group were injected intraperitoneally with 1.0 × 10² CFU of *ΔCRISPR_{S.a}-pSET2* or *ΔCRISPR_{S.a}-cadDX*. All the mice were euthanized at 24 h post-infection. Bacteria from the blood (**D**), brain (**E**), kidney (**F**), and liver (**G**) were plated onto THA, and colonies are expressed as Log₁₀ CFU/g or Log₁₀ CFU/mL. Data are presented as mean ± SD, and asterisks indicate significantly different values (**, ***, ****, and ***** indicate *p* < 0.05, *p* < 0.01, *p* < 0.001, and *p* < 0.0001, respectively).

these supplements are commonly used in modern swine farming practices [38]. It exerts toxicity by binding to sulfhydryl groups on essential proteins, inhibiting respiratory processes [39]. Moreover, cadmium also induces oxidative damage and weakens the survival capacity of microbes [40].

Among gram-positive bacteria, two common cadmium resistance systems are *cadDX* (also called *cadBX*) and *cadCA*, both of which are typically carried on plasmids. Within the plasmid pI258 of *S. aureus*, the *cadCA* system comprises a repressor, CadC, and an efflux protein, CadA. *S. aureus* CadC shares 35% amino acid identity

with *S. suis* CadX. The *cadC* gene encoded by the pI258 plasmid has been shown to bind metal ions, including Cd²⁺, Zn²⁺, lead (Pb²⁺), and bismuth (Bi³⁺), leading to derepression of the *cadCA* system [41, 42]. The *cadCA* system confers resistance to Cd²⁺, Zn²⁺, Pb²⁺, and Bi³⁺ in *S. aureus* [11, 43]. Unlike *S. aureus*, the *Listeria monocytogenes* plasmid pLm74 has a homologous *cadCA* system that specifically confers cadmium resistance [44]. The other system, *cadDX*, consists of the efflux protein CadD and the regulator protein CadX. In *S. lugdunensis*, the pLUG10 plasmid encodes CadX and CadD, which share 46% and 56% amino acid identity with *S. suis* CadX and

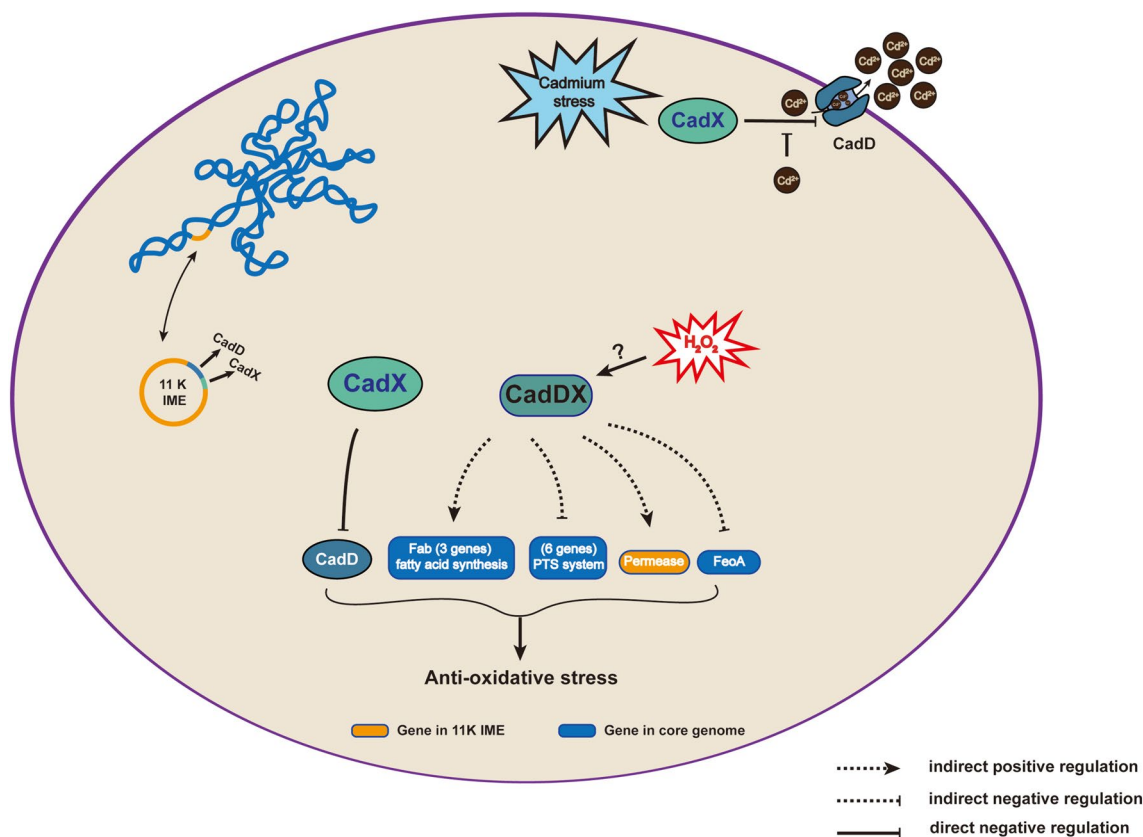


Figure 9 Functions and regulatory mechanisms of *cadDX*. In *S. suis*, *cadDX* is located within an 11K MGE that can autonomously form a circular structure. The presence of Cd^{2+} disrupts the repression of *cadD* by CadX, thereby contributing to cadmium resistance. CadX protects *S. suis* against oxidative stress by repressing *cadD* to prevent its excessive expression, which can be detrimental to the bacterium. Additionally, *cadDX* influences genes involved in the oxidative stress response, including fatty acid synthesis-related genes, PTS transport system-related genes, *permeases*, and *FeoA*, which contribute to oxidative stress resistance.

CadD, respectively [7]. The *cadDX* system in *S. lugdunensis* effectively contributes to resistance against Cd^{2+} [7]. In *S. salivarius*, CadDX, which shares 98% amino acid identity with that in *S. suis*, confers resistance to both Cd^{2+} and Zn^{2+} [12]. A recent study on *S. agalactiae* also demonstrated that CadD, which shares 98% amino acid identity with that in *S. suis*, contributes to tolerance to metal toxicity, including Zn^{2+} , Cd^{2+} , Cu^{2+} , Co^{2+} , and Ni^{2+} [13]. In this study, no observable effect of *cadDX* on zinc resistance was noted in *S. suis*. *S. suis* might rely on other compensatory resistance mechanisms to combat Zn^{2+} . Indeed, multiple zinc resistance mechanisms have been reported in *S. suis*. For example, Zheng et al. reported that TroR negatively regulates the *TroABCD* system, which is crucial for resistance to Zn^{2+} toxicity [25]. Another study demonstrated that AdcR negatively regulates the expression of *adcA* and *adcAII*, contributing to Zn^{2+} acquisition and virulence [45]. Furthermore, the Zn^{2+} -response regulator Zur plays a role in precise

Zn^{2+} homeostasis [46]. PmtA, which potentially affects the expression of the *Zur* regulon, is also involved in Zn^{2+} transport [24].

In addition to its role in conferring cadmium resistance, *cadDX* also plays a pivotal but previously unreported role in oxidative stress resistance. Oxidative stress, a common challenge faced by *S. suis* during infection, can damage cellular components by oxidizing amino acids, DNA, and lipids. In this study, we discovered that the *cadDX* operon, situated within the 11K IME, governs core genomic genes involved in resisting oxidative stress. The *FeoAB* system, a major ferrous iron transport system in pathogenic bacteria, is critical for intracellular survival and virulence [47, 48]. However, excessive intracellular ferrous iron can lead to the formation of hydroxyl radicals by reducing H_2O_2 in the Fenton reaction [49]. Hydroxyl radicals are highly potent oxidants of

cellular macromolecules [50]. Studies on *Porphyromonas gingivalis* and *Riemerella anatipestifer* have confirmed that knockout of *FeoAB* increases bacteria resistance to H₂O₂ stress [51, 52]. Our previous data also showed that *FeoAB* was downregulated in response to oxidative stress [35]. Therefore, it is possible that *cadDX* represses the expression of *FeoA* to protect *S. suis* against oxidative stress resulting from excessive intracellular ferrous iron. Furthermore, *cadDX* stimulates the expression of genes involved in fatty acid synthesis. Fatty acids are essential constituents of bacterial membranes [53, 54]. By modulating their membrane composition, bacteria can effectively respond to various environmental stresses, such as oxidative stress [55]. Our previous study demonstrated that *S. suis* curtails energy-consuming pathways to conserve energy for H₂O₂ detoxification [35]. In this study, *cadDX* might also inhibit energy-consuming pathways (six genes related to the PTS) to conserve energy for vital metabolic processes in the context of oxidative stress. Additionally, the permease of *Nitratiruptor* sp. SB155-2, which shares 41% amino acid identity with that of *S. suis*, was upregulated under cadmium or copper stress conditions [56], suggesting its potential role in maintaining metal homeostasis. Metal homeostasis is important for redox balance, so we speculated that *permeases* may also be involved in oxidative stress resistance. However, further investigations are needed to elucidate how the permease contributes to resistance against oxidative stress. The expression of *cadD* in the *C-cadD* strain was approximately 30-fold greater than that in the *C-cadDX* strain (Additional file 6A). The excessive expression of *cadD* may consume more ATP as an efflux pump, which is disadvantageous for combating oxidative stress. Additionally, excessive expression of *cadD* may disrupt metal homeostasis, leading to reduced resistance to H₂O₂ [57]. Thus, the repression of *cadD* by CadX is vital for combating oxidative stress. Notably, we determined that *cadX* harbors its own promoter and assists in combating oxidative stress by preventing the excessive expression of *cadD*. Furthermore, transcriptome analysis indicated that CadX may influence several genes involved in oxidative stress resistance, such as *permease*, *FeoA*, fatty acid synthesis-related genes, and PTS transport system-related genes, thereby contributing to oxidative stress resistance.

Our investigations revealed that *cadDX* is located within various MGEs, including IMEs, prophages, genomic islands, ICEs, and plasmids. This diversity of vectors implies that the *cadDX* operon has important implications for evolution and function within different bacterial populations, underscoring its

potential significance for bacterial adaptation and survival strategies.

In summary, as shown in Figure 9, in addition to investigating cadmium detoxification, we revealed new functions and regulatory mechanisms of the *cadDX* operon in oxidative stress resistance and virulence in *S. suis* and *S. agalactiae*. Furthermore, we identified the *cadDX* operon in diverse MGEs, accounting for its widespread distribution across various bacteria. These findings underscore the importance of the *cadDX* operon in shaping bacterial adaptation and survival strategies.

Supplementary Information

The online version contains supplementary material available at <https://doi.org/10.1186/s13567-024-01371-1>.

Additional file 1. Bacterial strains and plasmids used in this study.

Additional file 2. Primers used in this study.

Additional file 3. Information on *S. suis* strains with *cadDX*.

Additional file 4. Information on bacteria with *cadDX*.

Additional file 5. WT, Δ *cadDX*, *C-cadDX*, *C-cadD*, and *C-cadX* respond to zinc and copper stress. (A-D) Growth curves of the WT, Δ *cadDX*, *C-cadDX*, *C-cadD*, and *C-cadX* strains in THB supplemented with various concentrations of ZnCl₂ (0.25, 0.5, 1.0, and 2.0 mM). (E-H) Growth curves of the WT, Δ *cadDX*, *C-cadDX*, *C-cadD*, and *C-cadX* strains in THB supplemented with various concentrations of CuSO₄ (0.25, 0.5, 1.0, and 2.0 mM).

Additional file 6. *cadX* possesses its own promoter. (A) Expression of *cadD* in *C-cadDX* and *C-cadD*. Data are presented as mean \pm SD, and asterisks indicate significantly different values (**** indicates $p < 0.01$). (B) M: Molecular weight markers. Lines 1 and 3: 5'-RACE analysis using a reverse primer (GSP-*cadX*) designed to target *cadX*. Lines 2 and 4: 5'-RACE analysis using a reverse primer (NGSP-*cadX*) designed to target *cadX*. The amplification product indicated by the white arrow was subsequently purified, ligated into the pMD19T vector, and then sent for sequencing. (C) The sequence of the *cadDX* region in *S. suis* GZ0565. The double underline is the sequence including the *cadDX* operon promoter region in this study. The single underline is the sequence including the *cadX* promoter region in this study. The sequence marked in blue is the ORF of *cadD*. The sequence marked in green is the ORF of *cadX*. The single "G" with a red background is the additional TSS of *cadX*. (D) Analysis of the binding between CadX and its own promoter. (E) Activity of β -galactosidase under the control of the *cadX* promoter in the WT and Δ *cadDX* strains. Data are presented as mean \pm SD, and "ns" indicate no significantly different values.

Additional file 7. Differential gene expression in Δ *cadDX* compared with the WT.

Additional file 8. Validation of gene expression by RT-qPCR analysis. Seven upregulated and six downregulated DEGs were selected to confirm the reliability of the transcriptome data.

Additional file 9. Influence of the *cadDX* operon on the regulation of *S. suis* core genomic genes. (A-D) The activities of β -galactosidase under the control of the promoters of *Fab*, *permease*, *PTS*, and *FeoA* in the WT and Δ *cadDX* strains. Data are presented as mean \pm SD, and asterisks indicate significantly different values (**, ***, and **** indicate $p < 0.05$, $p < 0.01$, and $p < 0.001$, respectively). (E-H) CadX cannot bind to the promoter of *Fab*, *permease*, *PTS*, or *FeoA*.

Additional file 10. Permease and *FeoA* are involved in antioxidative stress. Survival rates of the WT, Δ *permease*, and OE-*FeoA* strains under H₂O₂ stress conditions. Data are presented as mean \pm SD, and asterisks indicate significantly different values (** and **** indicate $p < 0.05$ and $p < 0.01$, respectively).

Additional file 11. Bacterial loads of *S. agalactiae* strains in mouse spleens. Five mice per group were injected intraperitoneally with 1.0×10^2 CFU of Δ CRISPR_{S_o}-pSET2 or Δ CRISPR_{S_o}-cadDX. All the mice were euthanized at 24 h post-infection. Bacteria from the spleen were plated onto THA, and colonies were expressed as log₁₀CFU/g. Data are presented as mean \pm SD, and “ns” indicates no significant difference.

Acknowledgements

We thank Dr Daisuke Takamatsu for providing the pSET2 plasmid, Prof. Yongjie Liu for providing the *S. agalactiae* strains, and Prof. Zhe Ma for helpful discussions. This work was supported by the National Key Research and Development Program of China (No. 2021YFD1800402); the National Natural Science Foundation of China (No. 32172859); the Open Project Program of Jiangsu Key Laboratory of Zoonosis (No. R2103); and the Open Project Program of Engineering Research Center for the Prevention and Control of Animal Original Zoonosis, Fujian Province University (No. 2021ZW001).

Author's contributions

Data curation: XZ, ZW. Formal analysis: XZ, ZL, JM, ZW. Investigation: XZ, ZL, JH, LW, ZW. Project administration: HY, ZW. Supervision: ZW. Writing—original draft: XZ, ZW. Writing—review and editing: XZ, JM, JH, LW, ZW. All authors read and approved the final manuscript.

Availability of data and materials

The transcriptome data from this study have been deposited in the NCBI SRA database under the accession numbers SRR28595173, SRR28595174, SRR28595175, and SRR28595176.

Declarations

Competing interests

The authors declare that they have no competing interests.

Received: 1 July 2024 Accepted: 13 August 2024

Published online: 27 September 2024

References

- Whittle G, Shoemaker NB, Salyers AA (2002) The role of Bacteroides conjugative transposons in the dissemination of antibiotic resistance genes. *Cell Mol Life Sci* 59:2044–2054
- Shoemaker NB, Smith MD, Guild WR (1980) DNase-resistant transfer of chromosomal cat and tet insertions by filter mating in *Pneumococcus*. *Plasmid* 3:80–87
- Sullivan JT, Ronson CW (1998) Evolution of rhizobia by acquisition of a 500-kb symbiosis island that integrates into a phe-tRNA gene. *Proc Natl Acad Sci USA* 95:5145–5149
- Novick RP (2003) Mobile genetic elements and bacterial toxinoses: the superantigen-encoding pathogenicity islands of *Staphylococcus aureus*. *Plasmid* 49:93–105
- Johnson CM, Grossman AD (2015) Integrative and conjugative elements (ICEs): What they do and how they work. *Annu Rev Genet* 49:577–601
- McLellan LK, Anderson ME, Grossman AD (2022) Tn*Smu*1 is a functional integrative and conjugative element in *Streptococcus mutans* that when expressed causes growth arrest of host bacteria. *Mol Microbiol* 118:652–669
- Chaouni LB, Etienne J, Greenland T, Vandenesch F (1996) Nucleic acid sequence and affiliation of pLUG10, a novel cadmium resistance plasmid from *Staphylococcus lugdunensis*. *Plasmid* 36:1–8
- Nucifora G, Chu L, Misra TK, Silver S (1989) Cadmium resistance from *Staphylococcus aureus* plasmid pI258 cadA gene results from a cadmium-efflux ATPase. *Proc Natl Acad Sci USA* 86:3544–3548
- Gomez-Sanz E, Zarazaga M, Kadlec K, Schwarz S, Torres C (2013) Chromosomal integration of the novel plasmid pUR3912 from methicillin-susceptible *Staphylococcus aureus* ST398 of human origin. *Clin Microbiol Infect* 19:E519–522
- Fessler AT, Zhao Q, Schoenfelder S, Kadlec K, Brenner Michael G, Wang Y, Ziebuhr W, Shen J, Schwarz S (2017) Complete sequence of a plasmid from a bovine methicillin-resistant *Staphylococcus aureus* harbouring a novel ica-like gene cluster in addition to antimicrobial and heavy metal resistance genes. *Vet Microbiol* 200:95–100
- Endo G, Silver S (1995) CadC, the transcriptional regulatory protein of the cadmium resistance system of *Staphylococcus aureus* plasmid pI258. *J Bacteriol* 177:4437–4441
- Chen YY, Feng CW, Chiu CF, Burne RA (2008) cadDX operon of *Streptococcus salivarius* 57.1. *Appl Environ Microbiol* 74:1642–1645
- Korir ML, Doster RS, Lu J, Guevara MA, Spicer SK, Moore RE, Francis JD, Rogers LM, Haley KP, Blackman A, Noble KN, Eastman AJ, Williams JA, Damo SM, Boyd KL, Townsend SD, Henrique Serezani C, Aronoff DM, Manning SD, Gaddy JA (2022) *Streptococcus agalactiae* cadD alleviates metal stress and promotes intracellular survival in macrophages and ascending infection during pregnancy. *Nat Commun* 13:5392
- Goyette-Desjardins G, Auger JP, Xu J, Segura M, Gottschalk M (2014) *Streptococcus suis*, an important pig pathogen and emerging zoonotic agent—an update on the worldwide distribution based on serotyping and sequence typing. *Emerg Microbes Infect* 3:e45
- Ferrando ML, de Greeff A, van Rooijen WJ, Stockhofe-Zurwieden N, Nielsen J, Wichgers Schreur PJ, Pannekoek Y, Heuvelink A, van der Ende A, Smith H, Schultsz C (2015) Host-pathogen interaction at the intestinal mucosa correlates with zoonotic potential of *Streptococcus suis*. *J Infect Dis* 212:95–105
- Ferrando ML, Schultsz C (2016) A hypothetical model of host-pathogen interaction of *Streptococcus suis* in the gastro-intestinal tract. *Gut Microbes* 7:154–162
- Zaccaria E, Wels M, van Baaren P, Wells JM (2016) Temporal regulation of the transformosome and competence development in *Streptococcus suis*. *Front Microbiol* 7:1922
- Takamatsu D, Osaki M, Sekizaki T (2001) Construction and characterization of *Streptococcus suis*-*Escherichia coli* shuttle cloning vectors. *Plasmid* 45:101–113
- Dong Y, Ma K, Cao Q, Huang H, Nie M, Liu G, Jiang M, Lu C, Liu Y (2021) CRISPR-dependent endogenous gene regulation is required for virulence in piscine *Streptococcus agalactiae*. *Emerg Microbes Infect* 10:2113–2124
- Wu Z, Wu C, Shao J, Zhu Z, Wang W, Zhang W, Tang M, Pei N, Fan H, Li J, Yao H, Gu H, Xu X, Lu C (2014) The *Streptococcus suis* transcriptional landscape reveals adaptation mechanisms in pig blood and cerebrospinal fluid. *RNA* 20:882–898
- Langmead B, Salzberg SL (2012) Fast gapped-read alignment with Bowtie 2. *Nat Methods* 9:357–359
- Li B, Dewey CN (2011) RSEM: accurate transcript quantification from RNA-Seq data with or without a reference genome. *BMC Bioinformatics* 12:323
- Robinson MD, McCarthy DJ, Smyth GK (2010) edgeR: a Bioconductor package for differential expression analysis of digital gene expression data. *Bioinformatics* 26:139–140
- Zheng C, Jia M, Gao M, Lu T, Li L, Zhou P (2019) PmtA functions as a ferrous iron and cobalt efflux pump in *Streptococcus suis*. *Emerg Microbes Infect* 8:1254–1264
- Zheng C, Wei M, Qiu J, Jia M, Zhou X, Jiao X (2021) TroR negatively regulates the TroABCD system and is required for resistance to metal toxicity and virulence in *Streptococcus suis*. *Appl Environ Microbiol* 87:e0137521
- Peng W, Yang X, Wang Y, Wang N, Li X, Chen H, Yuan F, Bei W (2022) Mn uptake system affects the virulence of *Streptococcus suis* by mediating oxidative stress. *Vet Microbiol* 272:109518
- Yang X, Peng W, Wang Y, Yan K, Liu Z, Gao T, Yang K, Liu W, Guo R, Li C, Chen H, Tian Y, Zhou D, Bei W, Yuan F (2023) Mutations in troABCD against copper overload in a copA mutant of *Streptococcus suis*. *Appl Environ Microbiol* 89:e0184122
- Liu G, Gao T, Zhong X, Ma J, Zhang Y, Zhang S, Wu Z, Pan Z, Zhu Y, Yao H, Liu Y, Lu C (2020) The novel streptococcal transcriptional regulator XtgS negatively regulates bacterial virulence and directly represses PseP transcription. *Infect Immun* 88:e00035–e120
- Poyart C, Trieu-Cuot P (1997) A broad-host-range mobilizable shuttle vector for the construction of transcriptional fusions to beta-galactosidase in Gram-positive bacteria. *FEMS Microbiol Lett* 156:193–198
- Aviv G, Gal-Mor O (2018) lacZ reporter system as a tool to study virulence gene regulation in bacterial pathogens. *Methods Mol Biol* 1734:39–45

31. Sievers F, Wilm A, Dineen D, Gibson TJ, Karplus K, Li W, Lopez R, McWilliam H, Remmert M, Soding J, Thompson JD, Higgins DG (2011) Fast, scalable generation of high-quality protein multiple sequence alignments using Clustal Omega. *Mol Syst Biol* 7:539
32. Kumar S, Stecher G, Li M, Knyaz C, Tamura K (2018) MEGA X: molecular evolutionary genetics analysis across computing platforms. *Mol Biol Evol* 35:1547–1549
33. Segura M, Aragon V, Brockmeier SL, Gebhart C, Greeff A, Kerdsin A, O'Dea MA, Okura M, Salery M, Schultsz C, Valentin-Weigand P, Weinert LA, Wells JM, Gottschalk M (2020) Update on *Streptococcus suis* research and prevention in the Era of antimicrobial restriction: 4th International Workshop on *S. suis*. *Pathogens* 9:374
34. Lai L, Dai J, Tang H, Zhang S, Wu C, Qiu W, Lu C, Yao H, Fan H, Wu Z (2017) *Streptococcus suis* serotype 9 strain GZ0565 contains a type VII secretion system putative substrate EsxA that contributes to bacterial virulence and a vanZ-like gene that confers resistance to teicoplanin and dalbavancin in *Streptococcus agalactiae*. *Vet Microbiol* 205:26–33
35. Zhu X, Wang S, Du Y, Liang Z, Yao H, Chen X, Wu Z (2023) A novel aquaporin Aagp contributes to *Streptococcus suis* H₂O₂ efflux and virulence. *Virulence* 14:2249789
36. Guo CM, Chen RR, Kalhor DH, Wang ZF, Liu GJ, Lu CP, Liu YJ (2014) Identification of genes preferentially expressed by highly virulent piscine *Streptococcus agalactiae* upon interaction with macrophages. *PLoS ONE* 9:e87980
37. Kubier A, Pichler T (2019) Cadmium in groundwater—a synopsis based on a large hydrogeochemical data set. *Sci Total Environ* 689:831–842
38. Zhang F, Li Y, Yang M, Li W (2012) Content of heavy metals in animal feeds and manures from farms of different scales in northeast China. *Int J Environ Res Public Health* 9:2658–2668
39. Vallee BL, Ulmer DD (1972) Biochemical effects of mercury, cadmium, and lead. *Annu Rev Biochem* 41:91–128
40. Liu SH, Zeng GM, Niu QY, Liu Y, Zhou L, Jiang LH, Tan XF, Xu P, Zhang C, Cheng M (2017) Bioremediation mechanisms of combined pollution of PAHs and heavy metals by bacteria and fungi: a mini review. *Bioresour Technol* 224:25–33
41. Busenlehner LS, Weng TC, Penner-Hahn JE, Giedroc DP (2002) Elucidation of primary (α_3 N) and vestigial (α_2) heavy metal-binding sites in *Staphylococcus aureus* pl258 CadC: evolutionary implications for metal ion selectivity of ArsR/SmtB metal sensor proteins. *J Mol Biol* 319:685–701
42. Busenlehner LS, Apuy JL, Giedroc DP (2002) Characterization of a metal-oregulatory bismuth(III) site in *Staphylococcus aureus* pl258 CadC repressor. *J Biol Inorg Chem* 7:551–559
43. Yoon KP, Misra TK, Silver S (1991) Regulation of the cadA cadmium resistance determinant of *Staphylococcus aureus* plasmid pl258. *J Bacteriol* 173:7643–7649
44. Lebrun M, Audurier A, Cossart P (1994) Plasmid-borne cadmium resistance genes in *Listeria monocytogenes* are similar to cadA and cadC of *Staphylococcus aureus* and are induced by cadmium. *J Bacteriol* 176:3040–3048
45. Zheng C, Qiu J, Zhao X, Yu S, Wang H, Wan M, Wei M, Jiao X (2022) The AdcR-regulated AdcA and AdcAll contribute additively to zinc acquisition and virulence in *Streptococcus suis*. *Vet Microbiol* 269:109418
46. Feng Y, Li M, Zhang H, Zheng B, Han H, Wang C, Yan J, Tang J, Gao GF (2008) Functional definition and global regulation of Zur, a zinc uptake regulator in a *Streptococcus suis* serotype 2 strain causing streptococcal toxic shock syndrome. *J Bacteriol* 190:7567–7578
47. Lau CK, Krewulak KD, Vogel HJ (2016) Bacterial ferrous iron transport: the Feo system. *FEMS Microbiol Rev* 40:273–298
48. Sestok AE, Brown JB, Obi JO, O'Sullivan SM, Garcin ED, Deredge DJ, Smith AT (2022) A fusion of the *Bacteroides fragilis* ferrous iron import proteins reveals a role for FeoA in stabilizing GTP-bound FeoB. *J Biol Chem* 298:101808
49. Dubbs JM, Mongkolsuk S (2012) Peroxide-sensing transcriptional regulators in bacteria. *J Bacteriol* 194:5495–5503
50. Imlay JA (2003) Pathways of oxidative damage. *Annu Rev Microbiol* 57:395–418
51. Anaya-Bergman C, He J, Jones K, Miyazaki H, Yeudall A, Lewis JP (2010) *Porphyromonas gingivalis* ferrous iron transporter FeoB1 influences sensitivity to oxidative stress. *Infect Immun* 78:688–696
52. Huang M, Wang M, Feng Y, Wang M, Gao Q, Zhu D, Jia R, Chen S, Zhao X, Yang Q, Wu Y, Zhang S, Tian B, Huang J, Ou X, Mao S, Sun D, He Y, Wu Z, Cheng A, Liu M (2023) Functional characterization of FeoAB in iron acquisition and pathogenicity in *Riemerella anatipestifer*. *Microbiol Spectr* 11:e0137323
53. Fozo EM, Quivey RG Jr (2004) The fabM gene product of *Streptococcus mutans* is responsible for the synthesis of monounsaturated fatty acids and is necessary for survival at low pH. *J Bacteriol* 186:4152–4158
54. Lu YJ, Rock CO (2006) Transcriptional regulation of fatty acid biosynthesis in *Streptococcus pneumoniae*. *Mol Microbiol* 59:551–566
55. Cao X, van Putten JPM, Wosten M (2023) *Campylobacter jejuni* benefits from the bile salt deoxycholate under low-oxygen condition in a PldA dependent manner. *Gut Microbes* 15:2262592
56. Ares A, Sakai S, Sasaki T, Shimamura S, Mitarai S, Nunoura T (2022) Sequestration and efflux largely account for cadmium and copper resistance in the deep-sea *Nitratiruptor* sp. SB155-2 (phylum Campylobacterota). *Environ Microbiol* 24:6144–6163
57. Grunenwald CM, Choby JE, Juttukonda LJ, Beavers WN, Weiss A, Torres VJ, Skaar EP (2019) Manganese detoxification by MntE is critical for resistance to oxidative stress and virulence of *Staphylococcus aureus*. *MBio* 10:e02915–e2918

Publisher's Note

Springer Nature remains neutral with regard to jurisdictional claims in published maps and institutional affiliations.